

# DOCK10-Mediated Cdc42 Activation Is Necessary for Amoeboid Invasion of Melanoma Cells

Gilles Gadea,<sup>1</sup> Victoria Sanz-Moreno,<sup>1</sup> Annette Self,<sup>1</sup> Anna Godi,<sup>1</sup> and Christopher J. Marshall<sup>1,\*</sup>

<sup>1</sup>Cancer Research UK Centre for Cell and Molecular Biology  
Institute of Cancer Research  
237 Fulham Road  
London SW3 6JB  
United Kingdom

## Summary

**Background:** Tumor cells can move in a three-dimensional (3D) environment in either mesenchymal-type or amoeboid modes. In mesenchymal-type movement, cells have an elongated morphology with Rac-induced protrusions at the leading edge. Amoeboid cells have high levels of actomyosin contractility, and movement is associated with deformation of the cell body through the matrix without proteolysis. Because signaling pathways that control the activation of GTPases for amoeboid movement are poorly understood, we sought to identify regulators of amoeboid movement by screening an siRNA library targeting guanine nucleotide exchange factors (GEFs) for Rho-family GTPases.

**Results:** We identified DOCK10, a Cdc42 GEF, as a key player in amoeboid migration; accordingly, we find that expression of activated Cdc42 induces a mesenchymal-amoeboid transition and increases cell invasion. Silencing DOCK10 expression promotes conversion to mesenchymal migration and is associated with decreased MLC2 phosphorylation and increased Rac1 activation. Consequently, abrogating DOCK10 and Rac1 expression suppresses both amoeboid and mesenchymal migration and results in decreased invasion. We show that the Cdc42 effectors N-WASP and Pak2 are required for the maintenance of the rounded-amoeboid phenotype. Blocking Cdc42 results in loss of mesenchymal morphology, arguing that Cdc42 is also involved in mesenchymal morphology through different activation and effector pathways.

**Conclusions:** Previous work has identified roles of Rho and Rac signaling in tumor cell movement, and we now elucidate novel roles of Cdc42 signaling in amoeboid and mesenchymal movement and tumor cell invasion.

## Introduction

Recent studies of cell migration in three dimensions have led to a reassessment of the mechanisms that mediate tumor cell motility. In collagen gels, cell-derived matrices, slice cultures, and *in vivo*, cell movement and morphology may differ markedly from that seen on rigid planar substrata. A major difference between two-dimensional (2D) and three-dimensional (3D) environments is that in 3D, some tumor cells adopt an amoeboid form of movement that is not evident in 2D [1, 2]. Amoeboid movement is characterized by a rounded, blebbing morphology, independence from extracellular proteases, and a requirement for high levels of actomyosin contractility downstream of

RhoA-ROCK signaling to deform the extracellular matrix and propel cell movement [3–6]. Studies with intravital microscopy show that amoeboid movement of tumor cells can be very rapid *in vivo* (~5  $\mu\text{m}/\text{min}$  [7]). In contrast, mesenchymal-type movement can be seen in both 2D and 3D environments and is characterized by an elongated morphology, resulting from Rac-dependent actin assembly at the leading edge. These two modes of movement are interconvertible so that tumor cells may undergo amoeboid-mesenchymal and mesenchymal-amoeboid transitions [1, 4, 5]. This plasticity may permit adaptation of modes of migration in different environments.

Rho-family GTPases are key players in the signaling events for cell movement. Rac1 drives motility by promoting lamellipodium formation and cell protrusions [8]. RhoA signaling activates the ROCK family of kinases, promoting actin stress-fiber formation and generation of the actomyosin contractile force required for retraction of the rear of the cell in mesenchymal-type movement [9, 10]. High levels of RhoA-ROCK signaling generate cortical actin assembly and high levels of actomyosin contractility in amoeboid movement [3, 4]. Cdc42 is activated at the leading edge of lamellipodia and is required for Arp2/3-dependent actin assembly [11]. Cdc42 activation may also be required for Rac activation [12, 13]. In addition, Cdc42 has been shown to be important in generating directionality during mesenchymal movement through polarizing microtubules [14]. Although Cdc42 has been shown to be involved in cell motility in 2D, its role in 3D motility has not been investigated.

The regulation of Rho-family GTPase activity during cell movement is poorly understood. Guanine nucleotide exchange factors (Rho-family GEFs) control the activation of Rho-family GTPases [15], whereas GTPase-activating proteins (Rho-family GAPs) control inactivation. The human genome contains approximately 83 GEFs that fall into three subfamilies. The largest set is the DH-PH-containing proteins with Dbp as the prototype [16]; the DH domains mediate GEF activity, and the PH domains have an autoinhibitory role and may mediate membrane recruitment [17–19]. Rac, Rho, and Cdc42 have all been shown to be activated by DH-PH-domain-containing GEFs. Most members of the DH-PH family contain other interaction domains that connect the GEFs to signaling partners and cellular activities. Related to the DH-PH family is the small family of SWAP-70-related proteins in which a PH domain precedes a DH domain.

The second major class of GEFs is the DOCK family; these lack DH and PH domains, and exchange factor activity is mediated by DHR2 domains [20, 21]. Members of this family have high molecular mass (~200 kDa) and contain a second conserved domain, termed DHR1 [20, 21]. Unlike DH-PH-family GEFs, DOCK-family proteins are found in yeasts and plants as well as animals [20, 21]. DOCK-family members activate either Rac or Cdc42, and to date no member has been associated with Rho activation. DOCK180, as well as DOCK2 and DOCK3, activate Rac to regulate cell adhesion, cell spreading, migration, and phagocytosis [22–24]. The zizimin subfamily consists of three genes named zizimin1/DOCK9, zizimin2/DOCK11, and zizimin3/DOCK10. DOCK9 and DOCK11 are very similar and are exchange factors for Cdc42, but their tissue distribution in mice is different: DOCK9 is predominantly

\*Correspondence: [chris.marshall@icr.ac.uk](mailto:chris.marshall@icr.ac.uk)

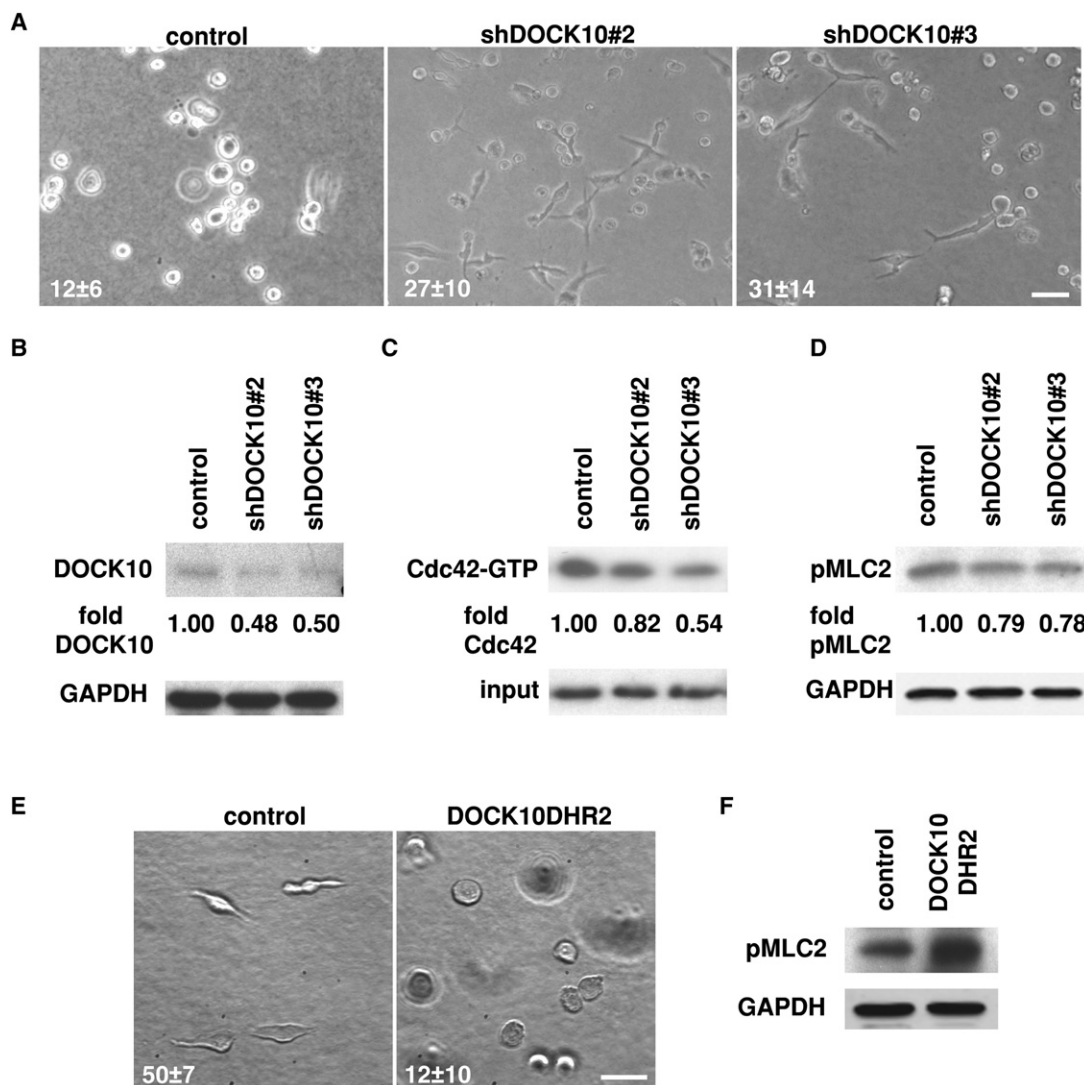


Figure 1. Cdc42 GEF DOCK10 Is Required for Rounded Morphology and Amoeboid Motility of A375M2 Melanoma Cells

(A) Still pictures taken at 24 hr of A375M2 cells stably expressing control or shRNA DOCK10 plated on thick collagen I in 1% serum and imaged with time-lapse phase-contrast microscopy (scale bar represents 100  $\mu$ m). The inset numbers show the percentage of cells with elongated morphology (>100 cells scored per experiment, n = 5, mean  $\pm$  SEM).

(B) Immunoblot showing knockdown of DOCK10.

(C) Levels of total and active GTP-bound Cdc42 from cells plated on a thick layer of collagen I. One representative experiment out of three is shown.

(D) Immunoblot for p-T18-S19-MLC2. One representative experiment out of three is shown.

(E) A375p cells expressing GFP-DOCK10DHR2 or GFP, plated on a thick layer of collagen I or embedded in collagen I in IBIDI chambers for 16 hr in 1% serum. IBIDI chambers were imaged with time-lapse phase-contrast microscopy for 3 hr. The inset numbers show the percentage of cells with elongated morphology (>100 cells scored per experiment, n = 3, mean  $\pm$  SEM).

(F) Immunoblot for p-T18-S19-MLC2. One representative experiment out of three is shown.

expressed in nonhematopoietic cells, and DOCK11 is predominantly expressed in lymphocytes [20, 25]. DOCK10 seems to be more widely expressed in mice, overlapping both DOCK9 and DOCK10 expression patterns, and appears to bind with a lower affinity to Cdc42 [25]. Interestingly, DOCK11 has been shown to mediate a positive feedback activation of Cdc42 [26].

Because nothing is known about the mechanisms underlying the activation of Rho-family GEFs in amoeboid movement, we set out to identify Rho-family GEFs required for amoeboid movement. Using siRNAs targeting 83 human Rho-family GEFs, we identified human DOCK10 acting in the regulation of amoeboid motility. This GEF is specific for amoeboid movement because when its expression is abrogated, cells undergo

an amoeboid-mesenchymal transition. DOCK10 targets Cdc42, and we show that the Cdc42 effectors N-WASP and Pak2 are required for amoeboid movement.

## Results

### Cdc42 GEF DOCK10 Is Required for Rounded Morphology and Amoeboid Motility of A375M2 Melanoma Cells

Amoeboid migration has been reported to be dependent on Rho-ROCK signaling and is associated with highly dynamic membrane blebbing driven by actomyosin contractility [4, 5, 27]. To identify GEFs that activate Rho-family GTPases required for amoeboid movement, we screened a library of siRNA

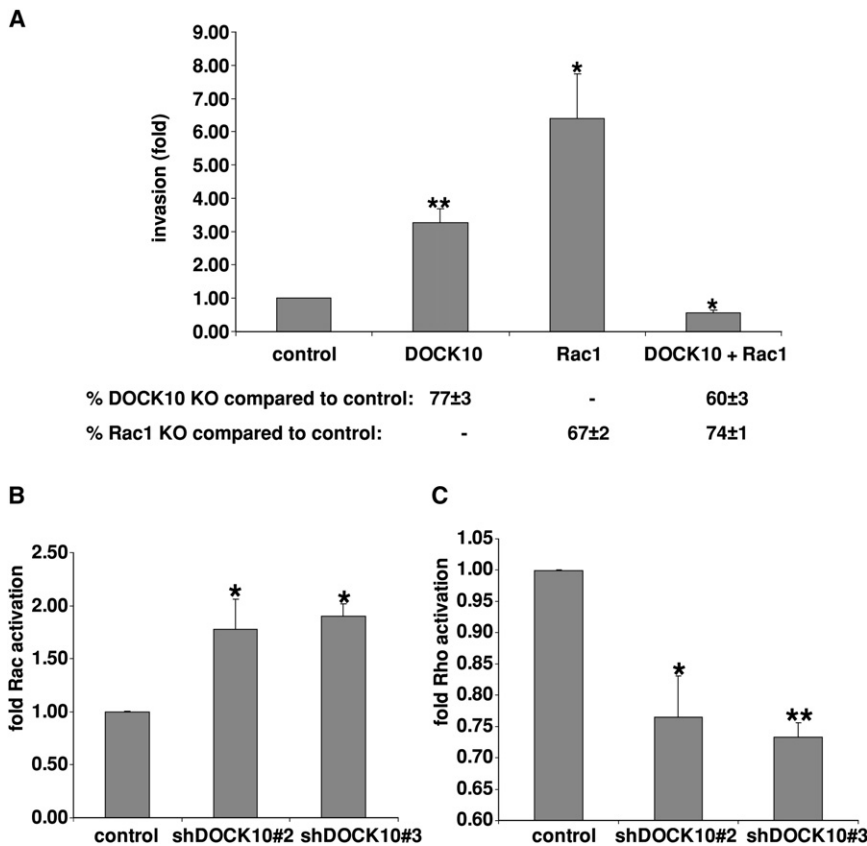


Figure 2. Simultaneous Blockade of DOCK10 and Rac Inhibits Tumor Cell Invasion

(A) Invasion into collagen I by A375M2 cells transfected with DOCK10, Rac1 siRNAs, or both together (n = 3, mean ± SEM). Knockdown of DOCK10 and Rac1 were estimated by Q-PCR. (B) Levels of active GTP-bound Rac1 from control and DOCK10 knockdown A375m2 stable cell lines plated on top of a thick layer of collagen I (n = 3, mean ± SEM). (C) Levels of active GTP-bound RhoA from cells on collagen I as for (B) (n = 3, mean ± SEM).

oligonucleotide duplexes targeting 83 RhoGEFs (Figure S1 available online) for their effects on amoeboid movement of A375M2 melanoma cells [4]. We used Dharmacon “SMART pools” in which each gene is targeted by siRNAs directed against four different sequences. The morphology and behavior of transfected cells was assessed on top of a thick layer of collagen I. In this assay, the majority of A375M2 cells have a rounded morphology with very dynamic blebbing plasma membranes, just as they do when they have invaded into a 3D collagen I matrix (Movie S1). This system therefore provides a way to screen for genes affecting membrane blebbing, cell morphology, and movement. Pools of siRNAs against five GEFs led to decreases in the number of cells with a rounded morphology and an increased proportion of elongated cells in three independent experiments (Figure S3A). Of these, Vav1 was not found to be expressed in A375M2 cells, whereas MCF2L2 and DOCK9 did not confirm with an independent set of siRNAs and appear to be off-target effects. Of the remaining two “hits,” DOCK6 and DOCK10, we focused on DOCK10 because it appeared to be involved in Cdc42 signaling [25] and the role of Cdc42 in amoeboid movement has not been studied [28]. Silencing DOCK10 with either the screening pool or five siRNAs targeting different regions of DOCK10 consistently resulted in cells adopting an elongated, polarized morphology and moving in a mesenchymal manner with long protrusions (Figures S3B and S3C). We also generated cell lines with stable knockdown of DOCK10 through expression of shRNAs that target different sequences from those used in the screen (Figure S3D). In two different DOCK10 shRNA cell lines (shDOCK10#2 and shDOCK10#3), the percentage of cells with elongated-mesenchymal morphology was 27% ± 10% (p value ≤ 0.04) and 31% ± 14% (p value ≤ 0.03) compared

to 12% ± 6% of elongated cells in the shRNA control cell line (Figure 1A and Movie S2). Figure 1B shows that DOCK10 protein levels are approximately 50% reduced in these cell lines. Tracking the motility of these elongated cells showed that they moved at  $0.211 \pm 0.026 \mu\text{m}/\text{min}$  (p value ≤ 0.01) and  $0.264 \pm 0.031 \mu\text{m}/\text{min}$  (p value ≤ 0.01) compared with  $0.109 \pm 0.008 \mu\text{m}/\text{min}$  for cells with a rounded morphology in A375M2 control populations. These results suggest that DOCK10 is required to maintain a rounded morphology and that loss of DOCK10 converts amoeboid movement to elongated-mesenchymal type. Screening a panel of melanoma cell lines shows that DOCK10

RNA is widely expressed but has a more variable expression than related family members DOCK9 and DOCK11 (Figure S4). Simultaneous knockdown of DOCK9, DOCK10, and DOCK11 produced no additional increase in the proportion of elongated cells over DOCK10 alone, arguing that DOCK10 acts nonredundantly (data not shown).

DOCK10 is a member of the zizimin subfamily in which DOCK9 and DOCK11 have been shown to be GEFs for Cdc42 [25, 29]. Therefore, we investigated Cdc42 activity in shRNA DOCK10 cell lines; Cdc42-GTP levels are decreased compared to those of control cell lines (shDOCK10#2: 0.67 ± 0.14-fold decrease, p value ≤ 0.02 and shDOCK10#3: 0.61 ± 0.13-fold decrease, p value ≤ 0.01), suggesting that DOCK10 acts as a Cdc42 GEF in vivo (Figure 1C). GEFs form stable complexes with their cognate GTPase in the nucleotide-free state, and we confirmed existing data indicating that DOCK10 binds to nucleotide-depleted Cdc42 but not Rac or Rho (Figure S5) [25]. Taken together, the observations that knockdown of DOCK10 results in decreased Cdc42-GTP and that DOCK10 binds nucleotide-free Cdc42 strongly argue that DOCK10 is a Cdc42 GEF.

High levels of phosphorylation of myosin light chain 2 (MLC2) are a feature of amoeboid motility [5]; therefore, we used phosphorylation of MLC2 as a biochemical marker of amoeboid behavior. As shown in Figure 1D, the knockdown of DOCK10 resulted in decreased MLC2 phosphorylation compared to control (shDOCK10#2: 0.74 ± 0.13-fold decrease, p value ≤ 0.03 and shDOCK10#3: 0.66 ± 0.19-fold decrease, p value ≤ 0.04), showing that DOCK10 signaling leads to elevated MLC2 phosphorylation.

Because abrogation of DOCK10 expression in A375M2 cells results in loss of amoeboid motility, we investigated whether

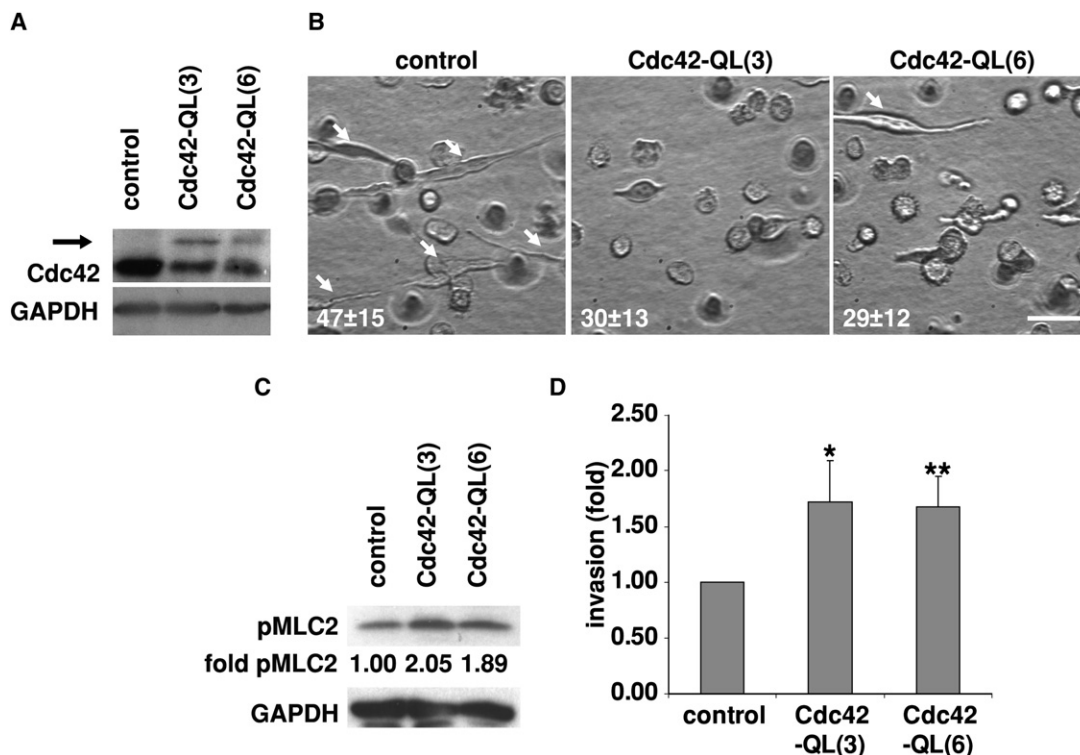


Figure 3. Activated Cdc42 Converts Mesenchymal-Type A375p Cells to Rounded Morphology and Increases Invasion

(A) Immunoblot of Cdc42 in A375p cells overexpressing Cdc42QL.

(B) Still pictures at end of 3 hr time-lapse video sequence of control or A375p cells stably expressing Cdc42-QL embedded in collagen I in IBIDI chambers (scale bar represents 100  $\mu$ m). Arrows point to elongated cells. The inset numbers show the percentage of cells with elongated morphology (>100 cells scored per experiment,  $n = 3$ , mean  $\pm$  SEM).

(C) Immunoblot for p-T18-S19-MLC2 from cells plated on a thick layer of collagen I. One representative experiment out of three is shown.

(D) Invasive properties of A375p cells expressing HA-tagged Cdc42-QL or control ( $n = 3$ , mean  $\pm$  SEM).

overexpressing DOCK10 in a mesenchymal-type cell line would lead to a rounded-amoeboid morphology. A375M2 cells were derived from A375p melanoma cells [30] that have a much higher proportion of elongated-mesenchymal cells with protrusions than A375M2 cells when plated on a thick layer of collagen I (50%  $\pm$  7% elongated cells versus 12%  $\pm$  6% for A375M2). When an N-terminally-truncated version of DOCK10 that retains the exchange factor DHR2 domain was expressed in A375p cells, the percentage of elongated-mesenchymal cells dropped dramatically to 12%  $\pm$  10% ( $p$  value  $\leq$  0.02) (Figure 1E). Consistent with the acquisition of a rounded-amoeboid morphology, expression of DOCK10DHR2 led to a strong increase in pMLC2 (Figure 1F). These data suggest that DOCK10 through increasing MLC2 phosphorylation can drive a rounded-amoeboid morphology.

#### Blocking DOCK10 and Rac1 Inhibits Tumor Cell Invasion

To examine the role of DOCK10 in invasion, we examined invasion into a 3D collagen I matrix. Figure 2A shows that knockdown of DOCK10 enhanced invasion by 3.27  $\pm$  0.42-fold ( $p$  value  $\leq$  0.01). This was somewhat surprising, however, given that we have observed that loss of DOCK10 resulted in increased motility of A375M2 cells with elongated-mesenchymal-type morphology. We investigated whether the increased invasion resulted from elevated levels of activated Rac1 that then drives mesenchymal-type movement. Figure 2B shows that when DOCK10 expression is reduced, there is increased Rac1-GTP compared to control (shDOCK10#2: 1.78  $\pm$  0.29-

fold increase in Rac-GTP,  $p$  value  $\leq$  0.04 and shDOCK10#3: 1.90  $\pm$  0.12-fold increase,  $p$  value  $\leq$  0.01). The increased Rac1 activation was associated with reduced activation of RhoA (Figure 2C; shDOCK10#2: 0.76  $\pm$  0.07-fold decrease in RhoA-GTP,  $p$  value  $\leq$  0.02 and shDOCK10#3: 0.73  $\pm$  0.02-fold decrease,  $p$  value  $\leq$  0.002); such an inverse relationship between Rac and Rho activity is well known [31]. Given these results, we tested whether the increased invasion in DOCK10 knockdown cells was dependent on Rac1. Silencing Rac1 and DOCK10 together abrogated the increase in invasion seen on silencing DOCK10 (0.56  $\pm$  0.08-fold decrease compared to control,  $p$  value  $\leq$  0.01). These results argue that in cells such as A375M2 that can interconvert between amoeboid and mesenchymal movement, DOCK10 and Rac1 act in different pathways. When DOCK10 cannot promote amoeboid movement, cells adopt Rac-dependent mesenchymal movement.

#### Activated Cdc42 Converts Mesenchymal-Type A375p Cells to Rounded Morphology and Increases Amoeboid Cell Movement and Invasion

These results suggest that activation of Cdc42 can lead to amoeboid motility and tumor cell invasion. Therefore, we examined whether expression of a constitutively active Cdc42 mutant (Cdc42-QL) in A375p cells would lead to conversion to a rounded morphology. Two different pools of cell lines with different levels of expression were isolated (Figure 3A). Cdc42-QL overexpression led to a higher proportion of cells with a rounded phenotype [Cdc42QL(3): 30%  $\pm$  13%

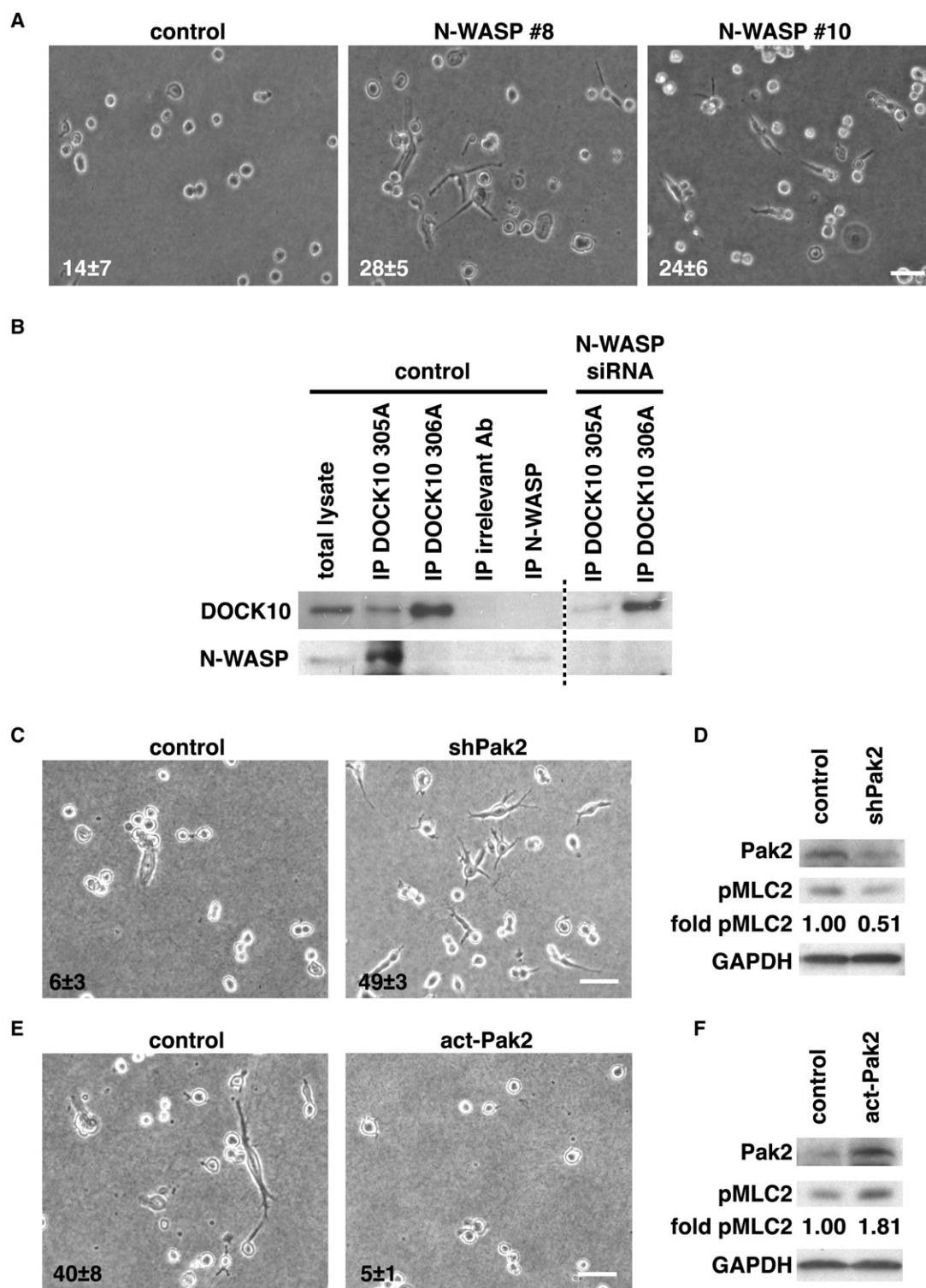


Figure 4. Cdc42 Effectors N-WASP and Pak2 Are Required for Rounded Morphology

(A) A375M2 cells transfected with control or N-WASP siRNAs plated on a thick layer of collagen I for 16 hr in 1% serum were time-lapsed for 24 hr. Still pictures from the end of the sequences are presented (scale bar represents 100  $\mu$ m). The inset numbers show the percentage of cells with elongated morphology (>100 cells scored per experiment, n = 5, mean  $\pm$  SEM).

(B) Coimmunoprecipitation of DOCK10 and N-WASP in WM1366. DOCK10 was immunoprecipitated with antibodies A301-305A (recognizing epitopes in aa 100–150) or A301-306A (aa 2136–2186) and immunoprecipitates blotted for N-WASP.

(C) Phase-contrast pictures from control or shPAK2 A375m2 cells plated on a thick layer of collagen I (scale bar represents 100  $\mu$ m). The inset numbers show the percentage of cells with elongated morphology (>100 cells scored per experiment, n = 3, mean  $\pm$  SEM).

(D) Immunoblots for Pak2 and p-T18-S19-MLC2. One representative experiment out of three is shown.

elongated cells,  $p$  value  $\leq 0.02$  and Cdc42QL(3):  $29\% \pm 12\%$  elongated cells,  $p$  value  $\leq 0.03$ ] compared to control A375p cells ( $47\% \pm 15\%$  elongated cells). Similar results were obtained with cells embedded in collagen I (Figure 3B and Movies S3 and S4). Figure 3C shows that these morphological changes were associated with increased MLC2 phosphorylation [Cdc42QL(3):  $1.70 \pm 0.41$ -fold increase,  $p$  value  $\leq 0.04$  and Cdc42QL(6):  $1.50 \pm 0.30$ -fold increase,  $p$  value  $\leq 0.05$ ]. This increased MLC2 phosphorylation appears to be Rho-kinase independent because ROCK inhibitor did not impair it (data not shown). We also analyzed the speed of amoeboid moving cells on top of a thick layer of collagen I by tracking cells with a round morphology. Cells overexpressing Cdc42-QL migrate significantly faster in an amoeboid manner [Cdc42QL(3):  $0.162 \pm 0.048$   $\mu\text{m}/\text{min}$ ,  $p$  value  $\leq 0.04$  and Cdc42QL(6):  $0.141 \pm 0.041$   $\mu\text{m}/\text{min}$ ,  $p$  value  $\leq 0.04$ ] than control amoeboid cells ( $0.079 \pm 0.017$   $\mu\text{m}/\text{min}$ ). To examine the role of Cdc42 in invasion, we tested invasion of control and Cdc42-expressing A375p into a collagen I matrix. Expression of activated Cdc42 increased tumor cell invasion compared to control [Figure 3D; Cdc42QL(3):  $1.89 \pm 0.41$ -fold increase,  $p$  value  $\leq 0.02$  and Cdc42QL(6):  $1.64 \pm 0.36$ -fold increase,  $p$  value  $\leq 0.04$ ]. These results show that activation of Cdc42 can enhance amoeboid movement and tumor cell invasion.

#### **Cdc42 Effectors N-WASP and Pak2 Promote Amoeboid Movement**

To identify effectors of Cdc42 signaling involved in amoeboid movement, we used siRNAs to screen a panel of Cdc42 effectors (listed in Figure S6). We found that silencing N-WASP or Pak2 had similar effects to those caused by silencing DOCK10. N-WASP knockdown in A375M2 led to the conversion toward a more elongated morphology; the percentage of elongated cells with two independent siRNAs was increased to  $28\% \pm 5\%$  ( $p$  value  $\leq 0.01$ ) and  $24\% \pm 6\%$  ( $p$  value  $\leq 0.01$ ), whereas the control had  $14\% \pm 7\%$  elongated cells (Figure 4A and Figure S7A). WASP-family proteins are key regulatory proteins of the actin cytoskeleton, with N-WASP mediating a direct connection between Cdc42 and the Arp2/3 complex for actin polymerization, and N-WASP has been shown to be important for cell migration [32, 33]. No change in MLC2 phosphorylation was observed after N-WASP knockdown (data not shown), suggesting that the Cdc42 effector N-WASP acts separately from high MLC2 phosphorylation to promote amoeboid movement.

Pak2 knockdown also led to an increased proportion of elongated cells (Figures 4C and Figures S7B–S7D). The p21-activated kinases (Paks) are a family of serine/threonine protein kinases, some of which, such as Pak2, bind and are stimulated by activated forms of Cdc42 and Rac [34]. Pak2 has been found to phosphorylate myosin light chain 2 downstream of Cdc42 and to induce contractility and endothelial cell retraction [35]. In Pak2 knockdown cell lines, MLC2 phosphorylation was decreased (Figure 4D,  $0.59 \pm 0.08$ -fold decrease compared to control,  $p$  value  $\leq 0.01$ ). To determine whether activated Pak2 could convert mesenchymal-type cells to a rounded morphology, we overexpressed activated Pak2 in A375p cells; Figures 4E and 4F show that overexpressing cells have a rounded amoeboid morphology and increased MLC2 phosphorylation ( $1.57 \pm 0.22$ -fold increase compared to

control,  $p$  value  $\leq 0.05$ ). These data demonstrate that the Cdc42 effector Pak2 can induce MLC2 phosphorylation and rounded morphology. To extend these data to another melanoma cell line, we examined the effects of knockdown of DOCK10, N-WASP, and Pak2 in WM1366 cells (Figure S8A). Similarly to A375M2, knockdown of DOCK10 and the two effectors increased the proportion of elongated cells (Figure S8B).

The idea that effectors bind to GEFs to provide selectivity in signaling is attractive [17]. To study whether there is evidence for interaction of DOCK10 with downstream effector pathways, we examined by coimmunoprecipitation whether DOCK10 interacts with N-WASP. Figure 4B shows that immunoprecipitating DOCK10 with an antibody A310-305A that recognizes epitopes within amino acids 100–150 of DOCK10 led to the detection of a complex containing DOCK10 and N-WASP. These results demonstrating that DOCK10 and N-WASP are in the same complex therefore provide a potential mechanism for selective signaling from Cdc42 to its effector N-WASP (Figure 4B). Antibody A310-306A recognizing epitopes within the C-terminal amino acids 2136–2186 did not immunoprecipitate a complex with N-WASP, presumably because these C-terminal epitopes are hidden within the complex and this antibody therefore only recognizes noncomplexed DOCK10.

#### **Cdc42 Inhibition Blocks Both Amoeboid and Mesenchymal Movement and Tumor Cell Invasion**

The data presented above show that increasing the activity of Cdc42 induces a mesenchymal-amoeboid transition. To further investigate the role of Cdc42 in amoeboid cells, we abrogated Cdc42 signaling in two ways: shRNA stable knockdown cell lines and dominant-negative Cdc42N17-expressing cells. Tracking movement of cells with a rounded morphology showed that in shRNA Cdc42 cells, there was a large decrease in speed ( $0.389 \pm 0.140$   $\mu\text{m}/\text{min}$  in control compared to  $0.133 \pm 0.043$   $\mu\text{m}/\text{min}$  in shCdc42 cells,  $p$  value  $\leq 0.02$ ). In A375M2 plated on a thick collagen I layer, there is always a small fraction of elongated cells. In Cdc42 shRNA and Cdc42N17 cells, the percentage of elongated cells was  $1\% \pm 1\%$  and  $4\% \pm 2\%$  compared with  $15\% \pm 3\%$  and  $13\% \pm 3\%$  for their respective controls ( $p$  values  $\leq 0.01$  and  $\leq 0.02$ ) (Figures 5A and 5C). These results suggest that Cdc42 is required not only for rounded morphology, but also for elongated-mesenchymal morphology. To further investigate the role of Cdc42 in elongated-mesenchymal morphology, we made use of the observation that treatment of A375M2 cells with a ROCK inhibitor increases the proportion of elongated cells [5]. Treatment of the scrambled shRNA control or HA-tag control cells increased the proportion of elongated cells to  $46\% \pm 9\%$  and  $42\% \pm 4\%$ , respectively, but in the shRNA Cdc42- or Cdc42N17-expressing cells, the proportion of elongated-mesenchymal cells after ROCK inhibitor treatment was only  $4\% \pm 2\%$  and  $17\% \pm 6\%$ , respectively ( $p$  values  $\leq 0.01$  and  $\leq 0.02$ ) (Figures 5A and 5C and Movies S5 and S6). These results with blocking Cdc42 signaling are in marked contrast to those found when expression of the Cdc42 GEF DOCK10 is abrogated, given that reducing the expression of DOCK10 increases the proportion of elongated cells (Figure 1). These observations suggest that Cdc42 is required for both

(E) Phase-contrast images of A375p cells stably expressing activated Pak2 or control vector plated on a thick layer of collagen I (scale bar represents 100  $\mu\text{m}$ ). The inset numbers show the percentage of cells with elongated-mesenchymal morphology (>100 cells scored per experiment,  $n = 3$ , mean  $\pm$  SEM). (F) Immunoblots for Pak2 and p-T18-S19-MLC2. One representative experiment out of three is shown.

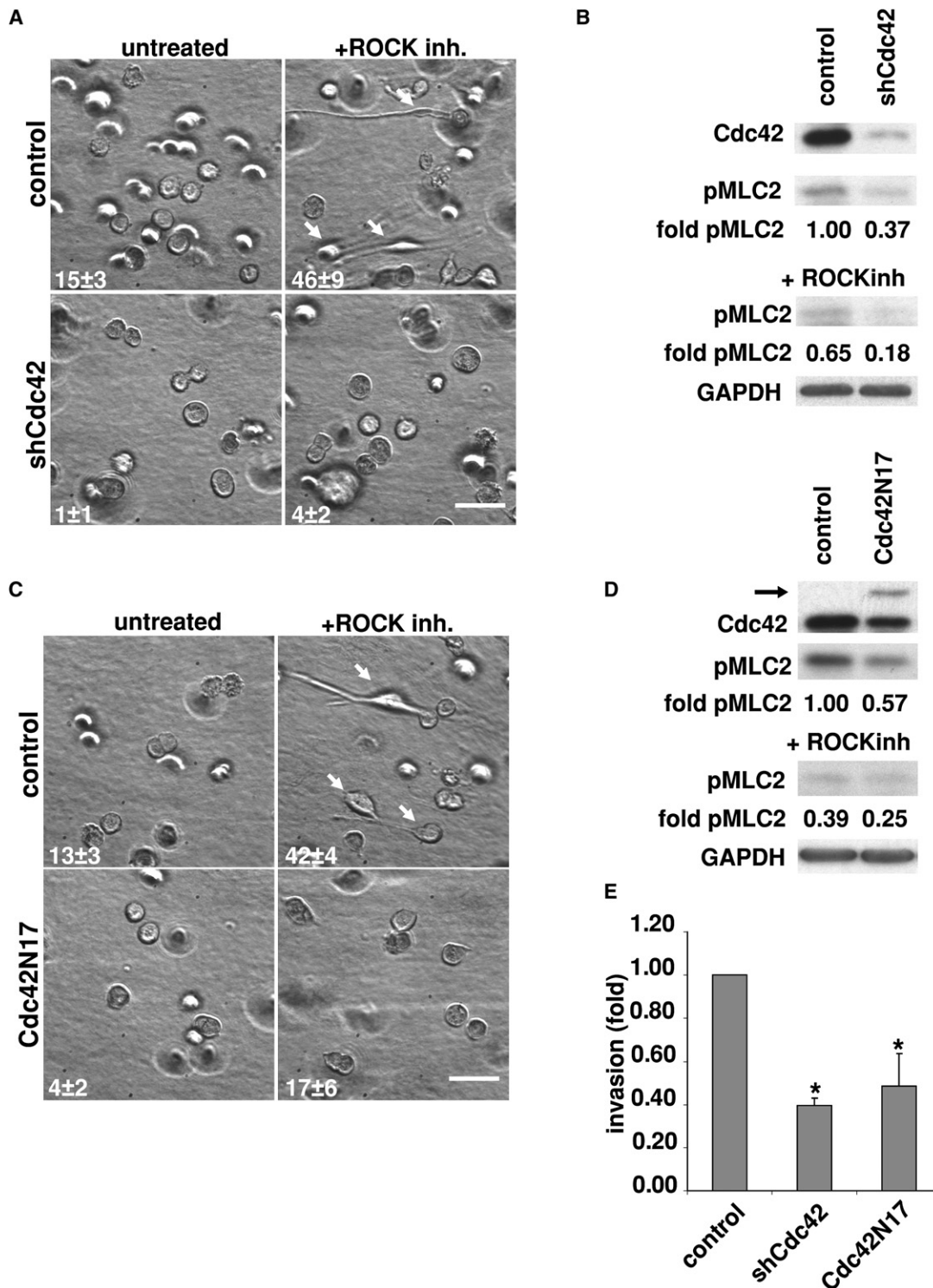


Figure 5. Cdc42 Inhibition Blocks Amoeboid-Mesenchymal Transition and Tumor Cell Invasion

(A) A375M2 cells with control vector or shRNA targeting Cdc42 were embedded in collagen I containing ROCK inhibitor or vehicle for 16 hr in IBIDI chambers, and then time-lapse movies were made for 3 hr. Still pictures are shown at 3 hr; arrows point to elongated cells (scale bar represents 100  $\mu$ m). The inset numbers show the percentage of cells with elongated morphology (>100 cells scored per experiment, n = 3, mean  $\pm$  SEM).

(B) Immunoblots for Cdc42 and p-T18-S19-MLC2. One representative experiment out of three is shown.

(C) A375M2 control cells or A375M2 cells expressing HA-tagged Cdc42N17 were embedded in collagen I containing ROCK inhibitor or vehicle for 16 hr in IBIDI chambers, and then time-lapse movies were made for 3 hr. Still pictures are shown from the end of the movies (scale bar represents 100  $\mu$ m). Arrows point to elongated cells. The inset numbers show the percentage of cells with elongated morphology (>100 cells scored per experiment, n = 3, mean  $\pm$  SEM).

(D) Immunoblots for Cdc42 and p-T18-S19-MLC2. One representative experiment out of three is shown.

(E) Invasion into collagen I (n = 3, mean  $\pm$  SEM).

amoeboid and mesenchymal morphology but that activation of Cdc42 by DOCK10 specifically acts in rounded morphology and amoeboid movement. Presumably, other Cdc42 GEFs are required for mesenchymal morphology and migration.

We have shown that DOCK10 signaling through Cdc42 contributes to actomyosin contractility through Pak2. However, Rho-Rho-kinase signaling is also known to contribute to MLC2 phosphorylation; therefore, we examined the relative contributions of Cdc42 and Rho-kinase signaling. Abrogation of Cdc42 signaling by RNAi knockdown or dominant-negative constructs resulted in a decrease of MLC2 phosphorylation (Figures 5B and 5D; ShCdc42QL:  $0.49 \pm 0.12$ -fold decrease,  $p$  value  $\leq 0.04$  and Cdc42N17:  $0.58 \pm 0.17$ -fold decrease,  $p$  value  $\leq 0.05$ ). Although treatment with ROCK inhibitor in control A375M2 cells did not completely block MLC2 phosphorylation, in cell lines in which Cdc42 signaling was blocked, ROCK inhibitor treatment led to an almost complete disappearance of MLC2 phosphorylation (Figures 5B and 5D; ShCdc42QL:  $0.21 \pm 0.04$ -fold decrease,  $p$  value  $\leq 0.01$  and Cdc42N17:  $0.18 \pm 0.07$ -fold decrease,  $p$  value  $\leq 0.01$ ). These results show that Cdc42 signaling makes multiple contributions to amoeboid morphology through N-WASP, Pak2, and MLC2 phosphorylation. Consistent with roles for Cdc42 in both amoeboid and mesenchymal movement, inhibition of Cdc42 results in a marked decrease in invasion compared to control (Figure 5E; ShCdc42:  $0.40 \pm 0.03$ ,  $p$  value  $\leq 0.01$ ).

## Discussion

The mammalian Rho GTPase family contains 22 members, but there are a much larger number of regulators, with more than 80 GEFs and more than 70 GAPs. An important concept is that signaling specificity is driven by specific GEFs, which may localize GTPase activity and lead to association with specific effectors through scaffolding and docking proteins [17]. We show that DOCK10 specifically controls Cdc42 activation in amoeboid motility of melanoma cells because silencing DOCK10 expression induces an amoeboid-mesenchymal transition. Interestingly, DOCK10 is implicated in tumor progression to a metastatic phenotype in other tumor types because a recent study that shows that DOCK10 is overexpressed in aggressive, poorly differentiated papillary thyroid carcinomas with extensive local invasion or synchronous distant metastases [36].

DOCK180, the prototypical member of the DOCK family, activates Rac downstream of integrins and contributes to mesenchymal movement. It is of interest that we show that a different member of the family, DOCK10, is linked to Cdc42 and amoeboid movement. DOCK10 is a member of the zizimin subfamily that may link Cdc42 activation to integrin signaling. Whether DOCK10 is involved in integrin signaling remains to be determined, but it is possible that it responds to other signals because studies from Friedl and coworkers have suggested that amoeboid movement is less dependent on integrin signaling than mesenchymal-type movement [2, 37]. Future studies will need to define how these GEFs are regulated, where they are located, and what are their transmembrane partners.

Our results identify a signaling module consisting of DOCK10-Cdc42-Pak2 that leads to the phosphorylation of MLC2. The evidence for this module is based on the following observations: Knockdown of DOCK10 results in reduced activation of Cdc42 and phosphorylation of MLC2; blocking Cdc42 or Pak2 signaling reduces MLC2 phosphorylation, whereas overexpression of the DOCK10 DHR2 domain or

activated versions of Cdc42 or Pak2 leads to increased MLC2 phosphorylation. These data present a strong argument for such a signaling pathway leading to increased actomyosin contractility, which results in a rounded morphology and amoeboid movement. Pak2 has been reported to control cell contractility by direct phosphorylation of MLC2 on serine 19 in endothelial cells [35]. However, we observed a decrease in both serine-19 and threonine-18 phosphorylation of MLC2 when Pak2 is inhibited. Whether Pak2 initiates the serine-19 phosphorylation followed by the consecutive phosphorylation of threonine 18 or Pak2 regulates a downstream kinase that is responsible for the diphosphorylation of MLC2 is not yet clear. Previous work from this laboratory has shown that the MRCK family of kinases downstream of Cdc42 can also contribute to actomyosin contractility through phosphorylation of the MYPT1-targeting subunit of myosin phosphatase [5], suggesting that Cdc42 has multiple inputs into the regulation of actomyosin contractility.

Working together with DOCK10-Cdc42-Pak2 signaling in amoeboid movement is DOCK10-Cdc42-N-WASP signaling. We show that there is a complex between N-WASP and DOCK10, supporting the idea that complexes between GEFs and effectors could provide specificity in signaling [17]. Although silencing N-WASP led to an elongated-mesenchymal morphology, it was not associated with a reduction in phospho-MLC2, arguing that N-WASP has a different role in amoeboid movement. N-WASP is well known to function in actin assembly [32]. As recently discussed by Fackler and Grosse [28], how actin is nucleated at the cell cortex during amoeboid movement is unclear, and our studies suggest that N-WASP could play such a role. However, Cdc42 signaling to N-WASP could have other roles, for example, in Golgi-to-ER protein transport required for amoeboid movement [38].

Our studies identify a Cdc42 activation and signaling pathway specific to amoeboid movement. However, we show that Cdc42 is also involved in mesenchymal-type movement. Abrogating the Cdc42 activator DOCK10 or the Cdc42 effectors Pak2 and N-WASP required for amoeboid movement leads to an elongated morphology. This argues that there are specific Cdc42 activation and effector pathways for elongated morphology and mesenchymal-type movement (see Figure 6). The identification of these pathways will be of considerable interest in delineating the differences in Cdc42 signaling pathways in the two modes of movement. In mesenchymal-type motility in 2D, Cdc42 is required for cell polarization toward the direction of the migration [14]. Additionally, a GEF-Cdc42-MRCK-mediated pathway leading to phosphorylation of MLC2 could also provide actomyosin contractility for mesenchymal-type movement [5]. Because it is clear that tumor cells can convert between different modes of movement, to inhibit tumor cell movement and block metastasis, it may be necessary to simultaneously inhibit both modes of movement or find components that are common to both pathways.

## Experimental Procedures

### Materials

Antibodies used include the following: anti-Cdc42 sc-8401 (Santa Cruz Biotechnology); anti-RhoA sc-418 (Santa Cruz Biotechnology); anti-Pak2 sc1872 (Santa Cruz Biotechnology); anti-DOCK10 A301-305A, A301-306A (Bethyl Laboratories); anti-Rac1 clone 23A8 (Upstate Biologicals); anti-diphospho-Thr18-Ser19-MLC2 (Cell Signaling Technology); anti- $\beta$ -Tubulin (Sigma-Aldrich); anti-N-WASP (Abcam), N-WASP 30D10 (Cell Signaling Technology); and anti-GAPDH (Novus Biologicals). Recombinant glutathione S-transferase (GST)-conjugated Rhotekin and Pak-CRIB were

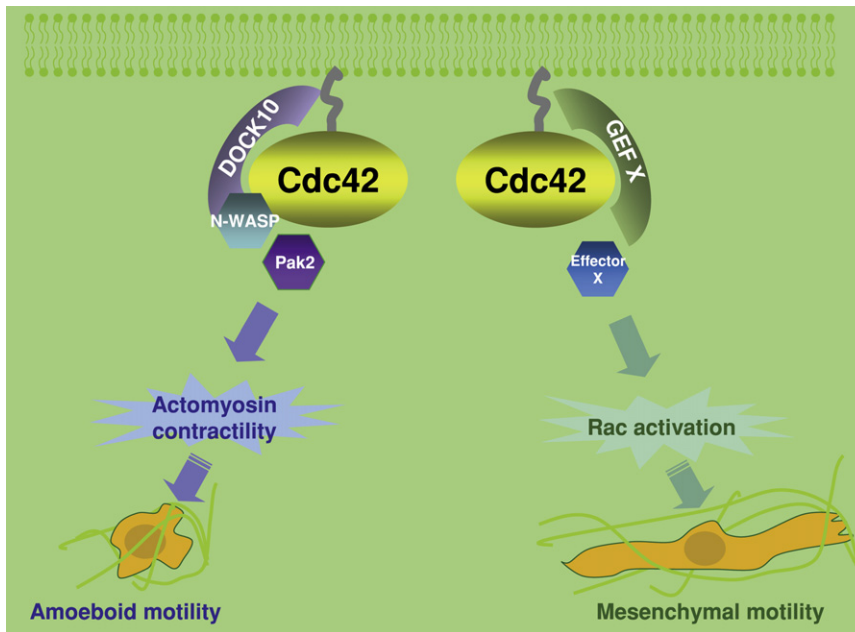


Figure 6. Schematic Representation of the Model

Model showing the contributions to amoeboid motility of DOCK10-Cdc42-N-WASP leading to actin assembly and DOCK10-Cdc42-Pak2 leading to actomyosin contractility; the model also shows a different Cdc42-dependent axis involving other GEFs and effectors that leads to Rac1 activation and elongated-mesenchymal-type motility.

collagen I (1.7 mg/ml) and loaded into the chamber (IBIDI). Cells were time-lapsed from 16 hr after setting of the collagen for 3 hr.

#### RNA Preparation, Reverse-Transcription, PCR, and Quantitative Real-Time One-Step PCR

RNA was prepared with RNeasy kits (QIAGEN). cDNAs were made with a First Strand cDNA Synthesis Kit from Amersham. PCRs were performed with DNA Taq polymerase from Sigma: Melting step was performed for 1 min at 95°C, annealing step for 30 s at 55°C, and elongation step for 30 s at 72°C, 28 cycles. The DOCK10 forward

primer was GATCTCTTGGAACTGAGTC, and the reverse was ATTCC TCTGGAAGTCCCCTTG. For analysis of DOCK10, DOCK9, and DOCK11 expression, Quantitect SYBR Green RT-PCR system (QIAGEN) was used according to the manufacturer's instructions.

#### Immunoprecipitation and Immunoblotting

For immunoprecipitation, cells were grown in 10 cm plates and lysed in 1% NP-40 buffer (1% NP-40, 150 mM NaCl, 50 mM Tris-HCl [pH 7.4], 25 mM sodium β-glycerophosphate, 1 mM sodium vanadate, 5 mM NaF, complete protease inhibitors [Roche 11-873-580-001]). Immunoprecipitations were carried out at 4°C for 3 hr on a rotating wheel. Immune complexes were precipitated with 25 μl of Protein G Agarose beads (Pierce) for 20 min on a rotating wheel at 4°C. After precipitation, beads were washed at least three times in 500 μl of lysis buffer and resuspended in Laemmli Sample Buffer prior to SDS PAGE.

2X Laemmli buffer lysates from a thick collagen I matrix (3 ml of collagen I preparation were set within a six-well dish) were fractionated by SDS-PAGE and transferred onto PVDF filters. Immunocomplexes were visualized by the ECL Plus Western Blotting Detection System (GE Healthcare-Amersham) with horseradish peroxidase-conjugated secondary antibodies (Sigma) or by fluorescence with the Li-COR Odyssey (Li-COR Biosciences). Fluorescence data from the Li-COR Odyssey were exported into Microsoft Excel.

#### Invasion Assays

Cells were resuspended in serum-free liquid bovine collagen I at 2.3 mg/ml for a final concentration of 10<sup>5</sup> cells/ml. 100 μl aliquots were then dispensed into black 96-well ViewPlates (Perkin-Elmer) previously coated with BSA. Plates were then centrifuged at 300 × g to force the cells toward the bottom of the wells and then incubated in a 10% CO<sub>2</sub> tissue culture incubator at 37°C. Once the collagen I had polymerized, 1% or 5% FCS was added on top of the collagen to promote invasion of the cells upwards into the collagen. After 24 hr incubation at 37°C in 10% CO<sub>2</sub>, cells were fixed and stained for 2 hr by adding 20% formaldehyde (Sigma) solution containing 5 μg/ml Hoechst 33258, a nuclear stain (Molecular Probes-Invitrogen); the final formaldehyde concentration was 4%. Plates were sealed with black tape to prevent evaporation and exposure to light. Confocal z slices were collected from each well at 40 μm for counting invaded cells and at the bottom of the wells (3 μm) for counting total cells with an INCELL3000 high-content microscope. Nuclear staining in each slice was quantified automatically by the INCELL3000 software with the Object Intensity module for determination of the percentage of invasive cells. Samples were run in quadruplicate and averaged.

#### Pull-Down Assays

For analysis of Cdc42, RhoA, and Rac1 activity, pull-down assays were performed as described previously [39], and where indicated, the extracts were

expressed from pGEX-Rhotekin and pGEX-CRIB. Y-27632 was from Tocris. H1152 was from Calbiochem (Merck Biosciences).

#### Cell Culture, Transfection, and Plasmids

A375p and A375M2 cells were a kind gift from R. Hynes (Howard Hughes Medical Institute, MIT, USA). Cells were routinely maintained in DMEM containing 10% fetal calf serum. Plasmid transfections were performed with Amaxa Nucleofector Transfection Reagent in accordance with the manufacturer's protocol (Amaxa). Stable cell lines were selected with G418 (Sigma). Y27632 was used at 10 μM and H1152 at 5 μM.

pCEFL-HA, -Cdc42-QL, and -Cdc42N17 were a kind gift from P. Crespo (University of Cantabria, Spain). EGFP-C1 was from Clontech, pRECEIVER-DOCK10DHR2-GFP was from Genecopoeia, and Sure Silencing shRNA plasmids for DOCK10, Cdc42, and Pak2 were from SuperArray (KH08298, KH00729N, and KH15598N, respectively). The control and constitutively active human Pak2 DNA constructs were obtained from J. Chernoff (Fox Chase Cancer Center, Philadelphia, PA, USA).

#### siRNA Transfections

siRNA oligonucleotide duplexes used were purchased from Dharmacon. The GEFs that were targeted are listed in Figure S1. Relevant oligonucleotide sequences are listed in Figure S2. For transfection, 2 × 10<sup>5</sup> cells were plated in a 30 mm dish overnight and transfected the next day with 20 nM SMART pools or individual oligos with Optimem-I and HiPerfect (QIAGEN). Cells were replated on collagen I in 1% serum at 48 hr and analyzed at 24–48 hr. Sequences of the relevant siRNA and shRNA oligonucleotides are listed in Figure S2.

#### Collagen Preparation, Time-Lapse Phase-Contrast Microscopy, Tracking Assays, and IBIDI Chambers

Fibrillar bovine dermal collagen I was prepared from a 1.7 mg/ml dilution in DMEM in accordance with the manufacturer's protocol (Cohesion); 300 μl was set within a 24-well plate. Time-lapse video microscopy of 24-well plates was performed in a humidified, CO<sub>2</sub>-equilibrated chamber with a Diaphot inverted microscope (Nikon) equipped with a motorized stage (Prior Scientific) controlled by Simple PCI software (Compix). Cells were tracked over a period of 24 hr from 16 hr after setting of the collagen I gel. Cells were tracked in a semiautomated manner by repeated random selection of cells in initial frames of time-lapse movies and tracing of migration pathways manually with Simple PCI analysis software (Compix). Path lengths were measured, and average cell speeds were derived for each cell by dividing the path length by the duration of the recording. For evaluation of the percentage of elongated cells, a cell was considered as elongated when its longest dimension was twice the shortest and when it showed at least one protrusion. For analysis of cells embedded in a 3D collagen matrix, cells were mixed with

derived from cells on a thick collagen I matrix (3 ml of collagen preparation was set within a six-well dish).

#### Supplemental Data

Supplemental Data include eight figures and six movies and can be found with this article online at <http://www.current-biology.com/cgi/content/full/18/19/1456/DC1/>.

#### Acknowledgments

We thank Imanol Arozarena for reagents, Kevin Harrington for cells, Pierfrancesco Marra and Hugh Paterson for advice, and Georgia Mavria, Pascal Peschard, and Harvey Smith for helpful comments. This work was supported by Cancer Research UK, a European Molecular Biology Organization long-term fellowship to G.G., and a Human Frontier Science Program fellowship to A.G. C.J.M. is a Gibb life fellow of Cancer Research UK.

Received: April 4, 2008

Revised: August 12, 2008

Accepted: August 12, 2008

Published online: October 2, 2008

#### References

- Friedl, P., and Wolf, K. (2003). Tumour-cell invasion and migration: Diversity and escape mechanisms. *Nat. Rev. Cancer* 3, 362–374.
- Wolf, K., Mazo, I., Leung, H., Engelke, K., von Andrian, U.H., Deryugina, E.I., Strongin, A.Y., Brocker, E.B., and Friedl, P. (2003). Compensation mechanism in tumor cell migration: Mesenchymal-amoeboid transition after blocking of pericellular proteolysis. *J. Cell Biol.* 160, 267–277.
- Wyckoff, J.B., Pinner, S.E., Gschmeissner, S., Condeelis, J.S., and Sahai, E. (2006). ROCK- and myosin-dependent matrix deformation enables protease-independent tumor-cell invasion in vivo. *Curr. Biol.* 16, 1515–1523.
- Sahai, E., and Marshall, C.J. (2003). Differing modes of tumour cell invasion have distinct requirements for Rho/ROCK signalling and extracellular proteolysis. *Nat. Cell Biol.* 5, 711–719.
- Wilkinson, S., Paterson, H.F., and Marshall, C.J. (2005). Cdc42-MRCK and Rho-ROCK signalling cooperate in myosin phosphorylation and cell invasion. *Nat. Cell Biol.* 7, 255–261.
- Sahai, E., Ishizaki, T., Narumiya, S., and Treisman, R. (1999). Transformation mediated by RhoA requires activity of ROCK kinases. *Curr. Biol.* 9, 136–145.
- Wyckoff, J.B., Jones, J.G., Condeelis, J.S., and Segall, J.E. (2000). A critical step in metastasis: In vivo analysis of intravasation at the primary tumor. *Cancer Res.* 60, 2504–2511.
- Ridley, A.J., Paterson, H.F., Johnston, C.L., Diekmann, D., and Hall, A. (1992). The small GTP-binding protein rac regulates growth factor-induced membrane ruffling. *Cell* 70, 401–410.
- Amano, M., Chihara, K., Kimura, K., Fukata, Y., Nakamura, N., Matsuura, Y., and Kaibuchi, K. (1997). Formation of actin stress fibers and focal adhesions enhanced by Rho-kinase. *Science* 275, 1308–1311.
- Kimura, K., Ito, M., Amano, M., Chihara, K., Fukata, Y., Nakafuku, M., Yamamori, B., Feng, J., Nakano, T., Okawa, K., et al. (1996). Regulation of myosin phosphatase by Rho and Rho-associated kinase (Rho-kinase). *Science* 273, 245–248.
- Ei-Sibai, M., Nalbant, P., Pang, H., Flinn, R.J., Sarmiento, C., Macaluso, F., Cammer, M., Condeelis, J.S., Hahn, K.M., and Backer, J.M. (2007). Cdc42 is required for EGF-stimulated protrusion and motility in MTLn3 carcinoma cells. *J. Cell Sci.* 120, 3465–3474.
- Nishimura, T., Yamaguchi, T., Kato, K., Yoshizawa, M., Nabeshima, Y., Ohno, S., Hoshino, M., and Kaibuchi, K. (2005). PAR-6-PAR-3 mediates Cdc42-induced Rac activation through the Rac GEFs STEF/Tiam1. *Nat. Cell Biol.* 7, 270–277.
- Baird, D., Feng, Q., and Cerione, R.A. (2005). The Cool-2/alpha-Pix protein mediates a Cdc42-Rac signaling cascade. *Curr. Biol.* 15, 1–10.
- Etienne-Manneville, S., and Hall, A. (2001). Integrin-mediated activation of Cdc42 controls cell polarity in migrating astrocytes through PKCzeta. *Cell* 106, 489–498.
- Nobes, C.D., and Hall, A. (1995). Rho, rac and cdc42 GTPases: Regulators of actin structures, cell adhesion and motility. *Biochem. Soc. Trans.* 23, 456–459.
- Hart, M.J., Eva, A., Evans, T., Aaronson, S.A., and Cerione, R.A. (1991). Catalysis of guanine nucleotide exchange on the CDC42Hs protein by the dbl oncogene product. *Nature* 354, 311–314.
- Schmidt, A., and Hall, A. (2002). Guanine nucleotide exchange factors for Rho GTPases: Turning on the switch. *Genes Dev.* 16, 1587–1609.
- Cerione, R.A., and Zheng, Y. (1996). The Dbl family of oncogenes. *Curr. Opin. Cell Biol.* 8, 216–222.
- Erickson, J.W., and Cerione, R.A. (2004). Structural elements, mechanism, and evolutionary convergence of Rho protein-guanine nucleotide exchange factor complexes. *Biochemistry* 43, 837–842.
- Meller, N., Irani-Tehrani, M., Kiosses, W.B., Del Pozo, M.A., and Schwartz, M.A. (2002). Zizimin1, a novel Cdc42 activator, reveals a new GEF domain for Rho proteins. *Nat. Cell Biol.* 4, 639–647.
- Cote, J.F., and Vuori, K. (2002). Identification of an evolutionarily conserved superfamily of DOCK180-related proteins with guanine nucleotide exchange activity. *J. Cell Sci.* 115, 4901–4913.
- Wu, Y.C., and Horvitz, H.R. (1998). C. elegans phagocytosis and cell-migration protein CED-5 is similar to human DOCK180. *Nature* 392, 501–504.
- Fukui, Y., Hashimoto, O., Sanui, T., Oono, T., Koga, H., Abe, M., Inayoshi, A., Noda, M., Oike, M., Shirai, T., et al. (2001). Haematopoietic cell-specific CDM family protein DOCK2 is essential for lymphocyte migration. *Nature* 412, 826–831.
- Namekata, K., Enokido, Y., Iwasawa, K., and Kimura, H. (2004). MOCA induces membrane spreading by activating Rac1. *J. Biol. Chem.* 279, 14331–14337.
- Nishikimi, A., Meller, N., Uekawa, N., Isobe, K., Schwartz, M.A., and Maruyama, M. (2005). Zizimin2: A novel, DOCK180-related Cdc42 guanine nucleotide exchange factor expressed predominantly in lymphocytes. *FEBS Lett.* 579, 1039–1046.
- Lin, Q., Yang, W., Baird, D., Feng, Q., and Cerione, R.A. (2006). Identification of a DOCK180-related guanine nucleotide exchange factor that is capable of mediating a positive feedback activation of Cdc42. *J. Biol. Chem.* 281, 35253–35262.
- Charras, G.T., Hu, C.K., Coughlin, M., and Mitchison, T.J. (2006). Reassembly of contractile actin cortex in cell blebs. *J. Cell Biol.* 175, 477–490.
- Fackler, O.T., and Grosse, R. (2008). Cell motility through plasma membrane blebbing. *J. Cell Biol.* 181, 879–884.
- Cote, J.F., and Vuori, K. (2006). In vitro guanine nucleotide exchange activity of DHR-2/DOCKER/CZH2 domains. *Methods Enzymol.* 406, 41–57.
- Clark, E.A., Golub, T.R., Lander, E.S., and Hynes, R.O. (2000). Genomic analysis of metastasis reveals an essential role for RhoC. *Nature* 406, 532–535.
- Sander, E.E., and Collard, J.G. (1999). Rho-like GTPases: Their role in epithelial cell-cell adhesion and invasion. *Eur. J. Cancer* 35, 1905–1911.
- Rohatgi, R., Ma, L., Miki, H., Lopez, M., Kirchhausen, T., Takenawa, T., and Kirschner, M.W. (1999). The interaction between N-WASP and the Arp2/3 complex links Cdc42-dependent signals to actin assembly. *Cell* 97, 221–231.
- Kowalski, J.R., Egile, C., Gil, S., Snapper, S.B., Li, R., and Thomas, S.M. (2005). Cortactin regulates cell migration through activation of N-WASP. *J. Cell Sci.* 118, 79–87.
- Sells, M.A., and Chernoff, J. (1997). Emerging from the Pak: The p21-activated protein kinase family. *Trends Cell Biol.* 7, 162–167.
- Zeng, Q., Lagunoff, D., Masaracchia, R., Goeckeler, Z., Cote, G., and Wysolmerski, R. (2000). Endothelial cell retraction is induced by PAK2 monophosphorylation of myosin II. *J. Cell Sci.* 113, 471–482.
- Fluge, O., Bruland, O., Akslen, L.A., Lillehaug, J.R., and Varhaug, J.E. (2006). Gene expression in poorly differentiated papillary thyroid carcinomas. *Thyroid* 16, 161–175.
- Friedl, P., Brocker, E.B., and Zanker, K.S. (1998). Integrins, cell matrix interactions and cell migration strategies: Fundamental differences in leukocytes and tumor cells. *Cell Adhes. Commun.* 6, 225–236.
- Luna, A., Matas, O.B., Martinez-Menarguez, J.A., Mato, E., Duran, J.M., Ballesta, J., Way, M., and Egea, G. (2002). Regulation of protein transport from the Golgi complex to the endoplasmic reticulum by CDC42 and N-WASP. *Mol. Biol. Cell* 13, 866–879.
- Sahai, E., and Marshall, C.J. (2002). ROCK and Dia have opposing effects on adherens junctions downstream of Rho. *Nat. Cell Biol.* 4, 408–415.